# Spatial dynamics of ecological public goods

Joe Yuichiro Wakano[a], Martin A. Nowak[b], and Christoph Hauert[c,1]

[a]Meiji Institute for Advanced Study of Mathematical Sciences, 1-1-1 Higashi Mita, Tama-ku, Kawasaki, Kanagawa 214-8571, Japan; [b]Program for Evolutionary Dynamics, Department of Organismic and Evolutionary Biology, Department of Mathematics, Harvard University, One Brattle Square, Cambridge, MA 02138; and [c]Department of Mathematics, University of British Columbia, 1984 Mathematics Road, Vancouver, BC, Canada V6T 1Z2

Edited by Richard E. Lenski, Michigan State University, East Lansing, MI, and approved March 16, 2009 (received for review December 11, 2008)

**The production, consumption, and exploitation of common resources ranging from extracellular products in microorganisms to global issues of climate change refer to public goods interactions. Individuals can cooperate and sustain common resources at some cost or defect and exploit the resources without contributing. This generates a conflict of interest, which characterizes social dilemmas: Individual selection favors defectors, but for the community, it is best if everybody cooperates. Traditional models of public goods do not take into account that benefits of the common resource enable cooperators to maintain higher population densities. This leads to a natural feedback between population dynamics and interaction group sizes as captured by ''ecological public goods.'' Here, we show that the spatial evolutionary dynamics of ecological public goods in ''selection-diffusion'' systems promotes cooperation based on different types of pattern formation processes. In spatial settings, individuals can migrate (diffuse) to populate new territories. Slow diffusion of cooperators fosters aggregation in highly productive patches (activation), whereas fast diffusion enables defectors to readily locate and exploit these patches (inhibition). These antagonistic forces promote coexistence of cooperators and defectors in static or dynamic patterns, including spatial chaos of ever-changing configurations. The local environment of cooperators and defectors is shaped by the production or consumption of common resources. Hence, diffusion-induced self-organization into spatial patterns not only enhances cooperation but also provides simple mechanisms for the spontaneous generation of habitat diversity, which denotes a crucial determinant of the viability of ecological systems.**

cooperation | evolutionary game theory | pattern formation | population dynamics

Spontaneous and complex pattern formation represents a common principle in physical, chemical, and biological systems ranging from hydrodynamical phenomena such as the ripples in the sand, to interacting chemical fronts (1), and the coloration of plants and animals such as the spots of the jaguar (2, 3), or vegetation patterns in arid ecosystems (4). Mathematical models of pattern formation use either cellular automata (5) or differential equations (6). Here, we show that similar types of patterns emerge in evolutionary settings of social dilemmas (7, 8). Social dilemmas are characterized by a conflict of interest between individuals and the group. Such conflicts arise in humans (9) and microorganisms alike (10–12). In antibiotic resistance, for example, bacteria secrete an enzyme that prevents cell wall degradation (11, 13, 14). Synthesizing the enzyme is costly to the bacterium, and releasing the enzyme creates a public good by protecting not only the bacterium itself but also the surrounding bacteria. Thus, enzyme production represents an act of cooperation that is prone to exploitation by mutant strains, which synthesize fewer or no enzymes. Such situations are captured by public-goods games (7, 15).

In a typical public-goods experiment, $N$ individuals have the opportunity to cooperate and invest a fixed amount, $c$, into a common pool or to defect and invest nothing. The total investment is multiplied by a factor, $r > 1$, and distributed equally among all participants—irrespective of whether they have invested or not. Thus, every invested unit returns $rc/N$ units to the investor (as well as to all other participants). Consequently, for $r < N$, rational players withhold their investments—but if all participants reason in this manner, the group foregoes the benefits of the public good, and no one receives anything. In contrast, had everybody cooperated, they would have been better off with a return of $(r - 1)c$. Conversely, if $r > N$ rational players invest in the public good (7) because, even with only a single investor, the return from the public goods exceeds the investment ($rc/N > c$).

In populations containing a fraction, $u$, of cooperators and a fraction, $v = 1 - u$, of defectors, the evolutionary dynamics can be described by the replicator equation (16): $\dot{u} = u(1 - u)(g_C - g_D)$. The fitness of cooperators and defectors, $g_C$, $g_D$, is determined by their performance in public-goods interactions in groups of size $N$ that are randomly formed according to binomial sampling. The average number of cooperators among the $N - 1$ interaction partners is $u(N - 1)$. Therefore, the average payoff of defectors is $g_D = u(N - 1)rc/N$, and of cooperators it is $g_C = g_D + rc/N - c$. Thus, $rc/N - c$ measures the effective cost of cooperation. For $r < N$, defectors win. For $r > N$, cooperators win. However, the replicator dynamics neglects the fact that cooperator populations have a higher productivity than defector populations. This should be reflected in the natural assumption that cooperators are capable of maintaining higher population densities than defectors.

## Model and Results

Ecological public goods allow the population density $u + v$ to fluctuate (17). This extension establishes a link between ecological and evolutionary dynamics. Variable population densities not only introduce feedbacks between reproductive success and carrying capacity but also affect the effective group size, $S$, in public-goods interactions. With $u + v \leq 1$, the densities $u$, $v$ can be interpreted in terms of probabilities when attempting to form interaction groups with $N$ participants [see supporting information (SI) *Text*]. In particular, each binomial sampling trial fails with probability $w = 1 - u - v$, such that the average interaction group size is reduced to $S = (u + v)N$. For $r < N$, this results in an interesting feedback, which enables cooperators and defectors to coexist: If population densities are high, interaction groups are large ($S > r$) and defectors increase, but this reduces the return from the public good and results in a decline of the population density. Decreasing population densities lead to smaller interaction groups until eventually $S < r$ holds, and cooperators thrive. This restores high population densities, and the cycle continues. Similar feedback mechanisms have been discussed in the complementary context of competitive interactions (18).

Author contributions: J.Y.W., M.A.N., and C.H. designed research; J.Y.W. and C.H. performed research; J.Y.W. contributed new reagents/analytic tools; J.Y.W. analyzed data; and J.Y.W., M.A.N., and C.H. wrote the paper.

The authors declare no conflict of interest.

This article is a PNAS Direct Submission.

[1]To whom correspondence should be addressed. E-mail: hauert@math.ubc.ca.

This article contains supporting information online at www.pnas.org/cgi/content/full/0812644106/DCSupplemental.

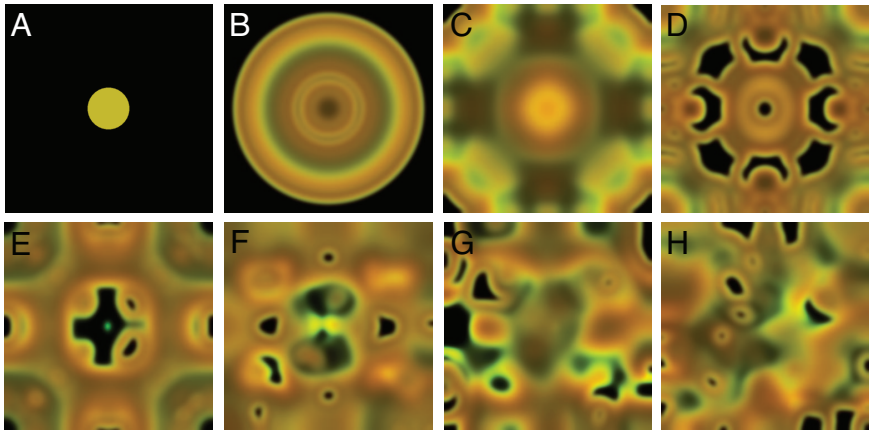


**Fig. 1.** Chaotic pattern formation in spatial ecological public goods. A sequence of snapshots *A*–*H* demonstrates the spatial density distribution of cooperators (green) and defectors (red) over time (see Movie S1). The symmetry of the initial configuration *A* should be preserved in a deterministic system, but after some time it breaks down and disappears because of limitations of the numerical integration of Eq. **2**. The exponential amplification of arbitrarily small disturbances characterizes chaotic systems. The initial configuration is a vacant $L \times L$ square ($L = 400$) with no flux boundaries and a homogeneous disk with radius $L/10$ in the center, where cooperators and defectors coexist at equal density ($u_{\text{disk}} = v_{\text{disk}} = 0.1$ and $u = v = 0$ elsewhere). The parameters of the ecological public goods are $N = 8$, $d = 1.2$, $b = 1$, $r = 2.34$, $c = 1$. The multiplication factor $r$ lies slightly below the Hopf bifurcation $r_{\text{Hopf}} = 2.3658$, such that the fixed point **Q** is unstable, and in the absence of space, the population disappears. Diffusion of defectors is twice that of cooperators ($D_{\text{C}} = 1$, $D_{\text{D}} = 2$). The color brightness indicates the density of cooperators (green) and defectors (red). The snapshots are taken at times $t = 0$ (*A*), 1,200 (*B*), 1,800 (*C*), 2,000 (*D*), 2,200 (*E*), 2,600 (*F*), 2,800 (*G*), 4,000 (*H*). The numerical integration uses a spatial grid with $dx = 0.8$ and step size $dt = 0.01$.

**Unstructured Populations.** The performance of cooperators and defectors in ecological public goods, $f_{\text{C}}, f_{\text{D}}$ (see *SI Text*), depends not only on the composition of the interaction groups but also on their size. Moreover, increasing population density exerts competitive pressure on the rates of reproduction, and the evolutionary dynamics become:

$$\dot{u} = u[w(f_C + b) - d] \qquad \textbf{[1a]}$$

$$\dot{v} = v[w(f_D + b) - d]. \qquad \textbf{[1b]}$$

Cooperators and defectors have an equal and constant per capita death rate, $d$, and a per capita birth rate of $w(f_{\text{C}} + b)$ and $w(f_{\text{D}} + b)$, which decreases for increasing population densities. The baseline birthrate, $b$, ensures $f_{\text{C}} + b \geq 0$ because $f_{\text{C}}$ can become negative in the limit $v \to 1$, which is not meaningful (17).

Hereafter, we assume that the death rate exceeds the baseline birth rate ($d > b$), such that defectors cannot survive in the absence of cooperators. However, cooperators and defectors can coexist at an equilibrium, **Q**, or exhibit rich population dynamics depending on $r$ (17). In particular, **Q** changes stability through a Hopf bifurcation at $r_{\text{Hopf}}$. For $r > r_{\text{Hopf}}$ coexistence in **Q** is stable but the basin of attraction limited. For unfavorable initial configurations, the returns from the public good are insufficient to offset the death rate, $d$, and the population goes extinct: At low densities, too few public-goods interactions occur, or, if defectors abound, exploitation irrecoverably diminishes the public resource. Generally, for $r < r_{\text{Hopf}}$, the equilibrium **Q** is unstable, and the population cannot survive (17).

**Spatial Dynamics.** To consider effects of spatial extension on the dynamics of ecological public goods, we introduce diffusive migration in 2 dimensions (19):

$$\dot{u} = D_C\nabla^2 u + u[w(f_C + b) - d] \qquad \textbf{[2a]}$$

$$\dot{v} = D_D\nabla^2 v + v[w(f_D + b) - d]. \qquad \textbf{[2b]}$$

The functions $u$, $v$ denote the density of cooperators and defectors at location $(x,y)$ and time $t$. As before, $w = 1 - u - v$ determines the negative feedback between population density and birth rates. The diffusion constants $D_{\text{C}}$ and $D_{\text{D}}$ specify the migration rates for cooperators and defectors and $\nabla^2$ denotes the diffusion operator. This continuous spatial extension reveals a fascinating world of dynamical pattern formation in ecological public goods [see Fig. 1, Fig. S1, Movie S1, Movie S2, Movie S3, and Movie S4, and interactive online tutorials Hauert C (2009) Virtuallabs: Interactive tutorials on evolutionary game theory, www.univie.ac.at/virtuallabs].

Spatial patterns unfold if defectors diffuse (migrate) faster than cooperators, $D_{\text{D}} \geq D_{\text{C}}$. Consequently, the dominant effect of spatial dynamics is not cooperators outrunning defectors but, instead, the defectors' relentless search of productive patches. Slow migration facilitates aggregation of cooperators, whereas fast migration supports defectors to readily locate cooperator patches, but it also impedes their ability to exploit one particular patch.

The equilibrium **Q** of Eq. **1** translates into a trivial solution of Eq. **2** in the form of a spatially homogeneous strategy distribution with densities according to **Q**. However, if **Q** is stable, this does not necessarily imply the stability of the corresponding homogeneous state. In the vicinity of **Q**, Eq. **2** takes on the form of an activator–inhibitor system. Any deviation from the equilibrium is amplified by cooperators (activators) but suppressed by defectors (inhibitors). For $D_{\text{D}} > D_{\text{C}}$, these antagonistic forces may give rise to the formation of complex patterns (Turing instability) (3, 6) (see Fig. 2*A*). Any small local disturbance propagates through the system and induces stable heterogeneous strategy distributions (see *SI Text*, Fig. S2, and Movie S3). Local disturbances may give rise to rearrangements of the patterns but then quickly relax into another qualitatively indistinguishable distribution of cooperators and defectors.

Conversely, if **Q** is unstable, then spatial extension and migration often prevents extinction and stabilizes coexistence of cooperators and defectors either in static spots and stripes similar to Turing patterns (see Fig. 2*B*) or in chaotic dynamics of ever-changing patterns (see Fig. 1 and Movie S1, Movie S2, and Movie S4). In general, a homogeneous population near **Q** exhibits periodic density oscillations of increasing amplitude that eventually result in extinction. However, any small local disturbance can propagate through space and trigger stationary, heterogeneous strategy distributions (see Fig. 2*B*). The pattern formation is again driven by the opposing forces of cooperators

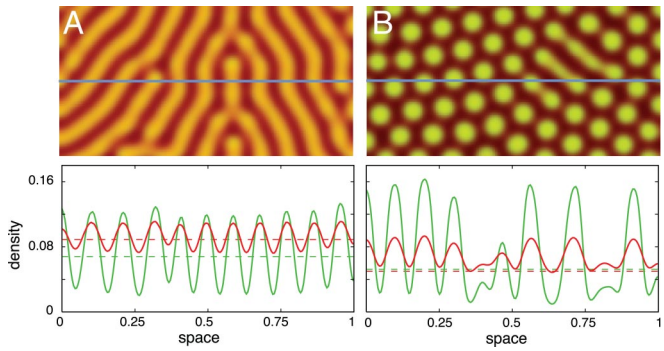


**Fig. 2.** Typical stationary patterns for diffusion-induced instability (Turing patterns) (*A*) and diffusion induced coexistence (*B*) on an $L \times L$ square (no flux boundaries). The density variation of cooperators (green) and defectors (red) is shown along a cross-section (solid blue line). (*A*) In the absence of space, cooperators and defectors coexist for suitable initial configurations ($r = 2.4 > r_{\mathrm{Hopf}} = 2.3658$). Diffusion destabilizes the spatially homogeneous state and induces stable and static heterogeneous strategy distributions, where individuals spontaneously aggregate in spots or striped patterns. (*B*) In the absence of space, the population goes extinct ($r = 2.24 < r_{\mathrm{Hopf}}$). Diffusion stabilizes persistence of the population and coexistence of cooperators and defectors by inducing heterogeneous strategy distributions. In both scenarios, the parameters of the ecological public goods are $n = 8$, $c = 1$, $d = 1.2$, $b = 1$, $D_{\mathrm{C}} = 1$, $D_{\mathrm{D}} = 10$, with an initial configuration where densities are randomly drawn in [0, 0.1]. Numerical integration is performed on a spatial grid with $L = 283$, $dx = 1.4$, and a step size of $dt = 0.1$. The brightness of the colors indicates the strategy densities (*Upper*) and the dashed horizontal lines mark the densities at **Q** (*Lower*).

(activators) and defectors (inhibitors). However, the activator–inhibitor system develops in the vicinity of an unstable fixed point (see *SI Text*, Fig. S3, and Movie S4), which could be termed "diffusion-induced coexistence" in contrast to the classical "diffusion-induced instability" of Turing patterns. Also note that, whereas Turing patterns rely on substantial differences in the diffusion constants of activators and inhibitors (see *SI Text* and Fig. S1), this does not apply to diffusion-induced coexistence, where dynamic patterns emerge even for $D_{\mathrm{D}} = D_{\mathrm{C}}$ (see Fig. 3).

## Discussion

In ecology, Turing patterns occur in spatial predator–prey models (20). Particularly rich dynamics develop in the vicinity of Turing–Hopf bifurcations (3, 21), as in the present case. Turing instabilities also occur in replicator–diffusion systems, but require at least 3 different strategic types (22). Two types are sufficient, however, if population densities can vary across space (23). In ecological public goods, cooperators and defectors suffice to produce rich spatiotemporal dynamics not only in the form of Turing patterns but also through diffusion-induced coexistence or deterministic chaos. Spatial dimensions generally support cooperation (24), and here, this holds in 3 different ways. First, the ratio of cooperators versus defectors is altered in favor of cooperators, which leads to an increase of the overall population density (see Fig. 4). Second, the robustness with respect to variations in the initial configuration is improved such that coexistence is much more easily achieved in spatial settings (see *SI Text* and Figs. S4–S6). Finally, and most importantly, spatial pattern formation based on diffusion-induced coexistence substantially extends the parameter range for the persistence of cooperators to settings where, otherwise, defectors would drive the population to extinction (see Figs. 3 and 4 for $r < r_{\mathrm{Hopf}}$).

Spatial games are traditionally based on 2 distinct types of discrete models that differ significantly from our approach. One type considers single individuals located in each site of a lattice or general network (25–28). Interactions are limited to a local neighborhood, and individuals are sedentary. Note that even small migration rates would severely challenge cooperation in these models. The other type of model considers metapopulations that consist of patches that are arranged on a lattice. Patches are linked to neighboring patches through migrating individuals (29–33). In the case of predator–prey interactions, this corresponds to a system of coupled oscillators that can exhibit highly complex dynamics (29–31). Our model represents a continuum limit of this second type of models, applied to the problem of cooperation.

The formulation in terms of continuous space based on partial differential equations (PDE) allows for a deeper understanding of the relevant mechanisms that drive the spontaneous generation of spatial heterogeneity and temporal fluctuations, which are ultimately responsible for supporting cooperation. Addition-

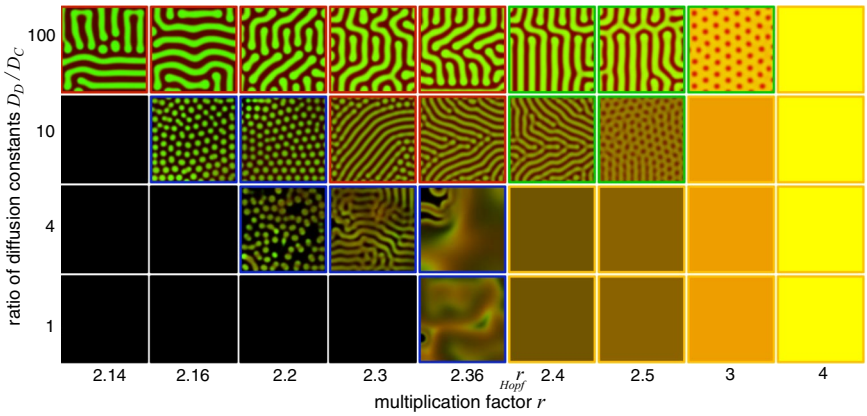


**Fig. 3.** Diversity of spatial distributions in terms of the ratio of the diffusion of defectors to cooperators $D_{\mathrm{D}}/D_{\mathrm{C}}$ and the multiplication factor $r$ in spatial ecological public-goods games. The brightness of the colors indicates the density of cooperators (green) and defectors (red). In the absence of space, the population survives for $r > r_{\mathrm{Hopf}}$. If cooperator diffusion exceeds defector diffusion, $D_{\mathrm{D}}/D_{\mathrm{C}} \leq 1$, the dynamics is barely affected by space, except for a small chaotic region (blue frame) near $r_{\mathrm{Hopf}}$. The dynamics becomes much richer for $D_{\mathrm{D}}/D_{\mathrm{C}} > 1$. For $r < r_{\mathrm{Hopf}}$, the chaotic regime increases (blue frame) and is replaced by diffusion induced coexistence patterns for high $D_{\mathrm{D}}/D_{\mathrm{C}}$ (red frame). For $r > r_{\mathrm{Hopf}}$, the homogeneous spatial distributions (orange frame) are replaced by diffusion-induced instability (Turing patterns; green frame) for high $D_{\mathrm{D}}/D_{\mathrm{C}}$. For very large $r$, all patterns disappear. The parameters are $N = 8$, $c = 1$, $d = 1.2$, $b = 1$, $D_{\mathrm{C}} = 1$, $L = 283$, $dx = 1.4$, $dt = 0.1$ ($r_{\mathrm{Hopf}} = 2.3658$) and an initial configuration with random cooperator and defector densities in [0, 0.1]. For a detailed phase plane diagram and other initial configurations see *SI Text* and Figs. S1 and S5.

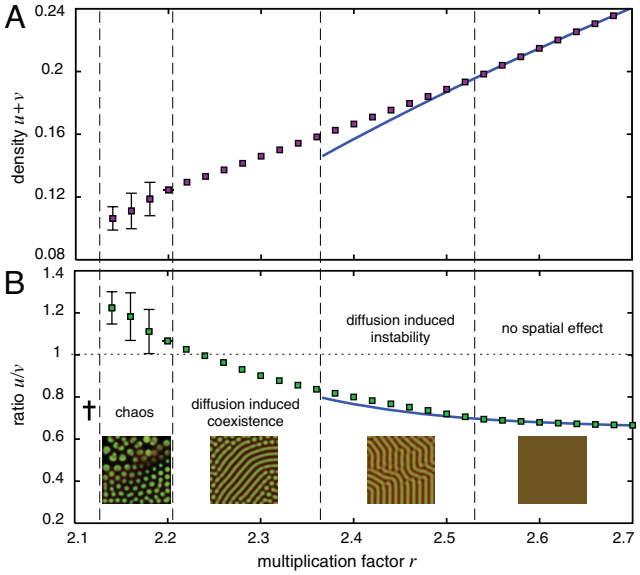


**Fig. 4.** Average global population density (*A*) and ratio of cooperators to defectors (*B*) as a function of the multiplication factor $r$ in ecological public-goods interactions. The nonspatial stable equilibrium (solid lines; requires $r > r_{Hopf}$) is shown together with numerical results for the stationary spatial distributions (dots). The chaotic regime depicts the average and standard deviation of the time series from $t = 5{,}000$ to 10,000 with $dt = 0.1$, $dx = 1.4$ and $L = 283$. For small $r$, the population goes extinct, but for increasing $r$, the population persists and exhibits chaotic dynamics that change into quasistatic and static patterns emerging through diffusion-induced coexistence ($r < r_{Hopf}$). For $r > r_{Hopf}$, static patterns are triggered by diffusion-induced instability (Turing patterns) and relax into spatially homogeneous coexistence for high $r$. Diffusion supports cooperation by significantly increasing the persistence region of the population and in the chaotic regime, cooperator densities even exceed those of defectors. Snapshots illustrate typical patterns emerging in the different dynamical regimes. The brightness of the colors indicates the density of cooperators (green) and defectors (red). The parameters for the ecological public goods game are $N = 8$, $c = 1$, $d = 1.2$, $b = 1$, $D_C = 1$, $D_D = 10$ such that $r_{Hopf} = 2.3658$.

ally, PDEs allow one to derive macroscopic quantities such as the relevant scale as well as the threshold for the onset of patterns emerging through Turing instabilities—features that are only empirically accessible in lattice models.

In our model, the local variability of the population density is a crucial feature combined with differences in migration rates of cooperators and defectors. The feedback between population density and interaction group size introduces a coupling of ecological and evolutionary dynamics, which enables cooperators to survive in well-mixed models (17). Fixing population densities at constant levels eliminates cooperation in both well-mixed and continuous spatial settings. In contrast to lattice models, continuous spatial extension alone is not enough to avert the extinction of cooperators, because diffusion prevents spatial segregation of cooperators and defectors, and hence, cooperators are unable to prevent exploitation by forming clusters. It is not merely the spatial dimensions but the emerging spatial heterogeneity that enables cooperators to persist at higher densities, or even more importantly, to survive under conditions that would inevitably result in the demise of the population otherwise.

Increased migration rates of defectors are motivated by the fact that defectors deplete common resources (or are unable to sustain them), and this causes them to move elsewhere. Conversely, migration rates of cooperators should be lower to enable them to take advantage of the locally sustained common resource.

In the context of antibiotic resistance, our results suggest that in spatial settings, susceptible free-riding strains (defectors) with high motility may actually increase the chances of survival as well as the density of the enzyme-producing, resistant strains (cooperators) and thereby aggravate the challenges for medical treatments. An interesting twist is introduced in microbial populations where migration rates or cell motility itself is linked to public-goods interactions. Examples include collective lubricant production in *Paenibacillus* to move across hard surfaces (34), the creation of an extracellular fibril matrix in *Myxococcus* to allow for cooperative swarming (12), or the formation of biofilms in *Pseudomonas* to gain competitive advantages in accessing limiting resources such as oxygen (10, 35). Particularly intriguing pattern formations are observed in *Escherichia coli* (36, 37). The chemotactic response to excreted aspartate amplifies spatial heterogeneity and enables cells to efficiently exploit available nutrients at the cost of producing the chemical signal. In the wake of the swarming cells, aggregates of sessile cells form. Cell aggregation may alleviate oxidative stress. Hence, in response to 2 common resources, nutrients and oxygen, *E. coli* strains diversify into 2 types with different motility (37).

Spatial heterogeneity supports coexistence (29, 30). In ecology, the most prominent example of pattern formation refers to the emergence of spatial vegetation patterns, which are usually associated with the risk of impending desertification (4, 38) because they indicate the ecosystems' bistability (39). Actually, the patterns stabilize the vegetated state, but environmental changes (absence of precipitation, overgrazing) may induce catastrophic shifts toward the desert state. In ecological public goods, similarly sharp transitions to extinction or homogeneous states are triggered by extreme external changes affecting the yield of the public resource.

Individuals consuming common resources, such as in Hardin's *Tragedy of the commons* (8), or producing common resources may alter and shape their environment in an enduring manner. This is particularly evident in microbial systems involving extracellular products such as in antibiotic resistance (11, 13, 14), biofilms (10), or swarming (12) and represent crucial determinants of microbial ecology (40). Spatial ecological public goods model concurrent spontaneous habitat diversification and species coexistence and hence suggest a mechanism to promote biodiversity (30, 41).

**ACKNOWLEDGMENTS.** J.Y.W. acknowledges support from Japanese Science Foundation Grant JSPS.KAKENHI 18-09976. M.A.N. and C.H. acknowledge support from the John Templeton Foundation and the National Science Foundation/National Institutes of Health (NIH) joint program in mathematical biology (NIH Grant R01GM078986). C.H. acknowledges support from the Natural Sciences and Engineering Research Council of Canada.

1. Lee KJ, McCormick WD, Ouyang Q, Swinney HL (1993) Patterns formation by interacting chemical fronts. *Science* 261:192–194.
2. Gell-Mann, M (1994) *The Quark and the Jaguar: Adventures in the Simple and the Complex* (Freeman, New York).
3. Pearson JE (1993) Complex patterns in a simple system. *Science* 261:189–192.
4. Rietkerk M, Dekker SC, de Ruiter PC, van de Koppel J (2004) Self-organized patchiness and catastrophic shifts in ecosystems. *Science* 305:1926–1929.
5. Wolfram S, ed (1986) *Theory and Applications of Cellular Automata* (World Scientific, Singapore).
6. Turing AM (1952) The chemical basis of morphogenesis. *Philos Trans R Soc London Ser B* 237:37–72.
7. Hauert C, Michor F, Nowak M, Doebeli M (2006) Synergy and discounting of cooperation in social dilemmas. *J Theor Biol* 239:195–202.
8. Hardin G (1968) The tragedy of the commons. *Science* 162:1243–1248.
9. Milinski M, Semmann D, Krambeck HJ, Marotzke M (2006) Stabilizing the earth's climate is not a losing game: Supporting evidence from public goods experiments. *Proc Natl Acad Sci USA* 103:3994–3998.
10. Rainey PB, Rainey K (2003) Evolution of cooperation and conflict in experimental bacterial populations. *Nature* 425:72–74.
11. Neu HC (1992) The crisis in antibiotic resistance. *Science* 257:1064–1073.
12. Velicer GJ, Yu YTN (2003) Evolution of novel cooperative swarming in the bacterium *Myxococcus xanthus*. *Nature* 425:75–78.

13. Lenski RE, Hattingh SE (1986) Coexistence of two competitors on one resource and one inhibitor: A chemostat model based on bacteria and antibiotics. *J Theor Biol* 122:83–93.
14. Dugatkin LA, Perlin M, Lucas JS, Atlas R (2005) Group-beneficial traits, frequency-dependent selection and genotypic diversity: An antibiotic resistance paradigm. *Proc R Soc London Ser B* 272:79–83.
15. Kagel JH, Roth AE, eds (1995) *The Handbook of Experimental Economics* (Princeton Univ Press, Princeton).
16. Hofbauer J, Sigmund K (1998) *Evolutionary Games and Population Dynamics* (Cambridge Univ Press, Cambridge, UK).
17. Hauert C, Wakano JY, Doebeli M (2008) Ecological public goods games: Cooperation and bifurcation. *Theor Pop Biol* 73:257–263.
18. Rankin DJ (2007) Resolving the tragedy of the commons: The feedback between intraspecific conflict and population density. *J Evol Biol* 20:173–180.
19. Wakano JY (2006) A mathematical analysis on public goods games in the continuous space. *Math Bio Sci* 201:72–89.
20. Mimura M, Murray J (1978) On a diffusive prey-predator model which exhibits patchiness. *J Theor Biol* 75:249–262.
21. Baurmann M, Gross T, Feudel U (2007) Instabilities in spatially extended predator–prey systems: Spatio-temporal patterns in the neighborhood of Turing–Hopf bifurcations. *J Theor Biol* 245:220–229.
22. Vickers GT, Hutson VCL, Budd CJ (1993) Spatial patterns in population conflicts. *J Math Biol* 31:411–430.
23. Cressman R, Vickers GT (1997) Spatial and density effects in evolutionary game theory. *J Theor Biol* 184:359–369.
24. Doebeli M, Hauert C (2005) Models of cooperation based on the prisoner's dilemma and the snowdrift game. *Ecol Lett* 8:748–766.
25. Nowak MA, May RM (1992) Evolutionary games and spatial chaos. *Nature* 359:826–829.
26. Ohtsuki H, Hauert C, Lieberman E, Nowak MA (2006) A simple rule for the evolution of cooperation on graphs and social networks. *Nature* 441:502–505.
27. Szabó G, Fáth G (2007) Evolutionary games on graphs. *Phys Rep* 446:97–216.
28. Taylor PD, Day T, Wild G (2007) Evolution of cooperation in a finite homogeneous graph. *Nature* 447:469–472.
29. Hassell MP, Comins HN, May RM (1991) Spatial structure and chaos in insect population dynamics. *Nature* 353:255–258.
30. Hassell MP, Comins HN, May RM (1994) Species coexistence and self-organizing spatial dynamics. *Nature* 370:290–292.
31. Jansen VAA, Sigmund K (1998) Shaken not stirred: On permanence in ecological communities. *Theor Pop Biol* 54:195–201.
32. Alizon S, Taylor P (2008) Empty sites can promote altruistic behavior. *Evolution (Lawrence, Kans)* 62:1335–1344.
33. Sella G, Lachmann M (2000) On the dynamic persistence of cooperation: How lower individual fitness induces higher survivability. *J Theor Biol* 206:465–485.
34. Ben-Jacob E, Levine H (2006) Self-engineering capabilities of bacteria. *J R Soc Interface* 3:197–214.
35. Xavier JB, Foster KR (2007) Cooperation and conflict in microbial biofilms. *Proc Natl Acad Sci USA* 104:876–881.
36. Budrene EO, Berg HC (1991) Complex patterns formed by motile cells of *Escherichia coli*. *Nature* 349:630–633.
37. Budrene EO, Berg HC (1995) Dynamics of formation of symmetrical patterns by chemotactic bacteria. *Nature* 376:49–53.
38. Scanlon TM, Caylor KK, Levin SA, Rodriguez-Iturbe I (2007) Positive feedbacks promote power-law clustering of Kalahari vegetation. *Nature* 449:209–212.
39. von Hardenberg J, Meron E, Shachak M, Zarmi Y (2001) Diversity of vegetation patterns and desertification. *Phys Rev Lett* 87:198101.
40. Prosser JI, et al. (2007) The role of ecological theory in microbial ecology. *Nat Rev Microbiol* 5:384–392.
41. Tilman D, Reich PB, Knops JMH (2006) Biodiversity and ecosystem stability in a decade-long grassland experiment. *Nature* 441:629–632.

# Supporting Information

Wakano et al. 10.1073/pnas.0812644106

## SI Text

**Model Analysis.** Consider the following selection–diffusion dynamics for the density of cooperators, $u(x, y, t)$, and defectors, $v(x, y, t)$, as a function of the spatial coordinates $x$, $y$, and time $t$:

$$\partial_t u = D_C \nabla^2 u + u[w(f_C + b) - d] \quad \text{[S1a]}$$

$$\partial_t v = D_D \nabla^2 v + v[w(f_D + b) - d] \quad \text{[S1b]}$$

The per capita birth rate of cooperators and defectors, $w(f_C + b)$ and $w(f_D + b)$, is determined by the baseline birthrate, $b$, their performance in public-goods interactions, $f_C$ and $f_D$, respectively, and is negatively correlated with the population density $u + v$ through $w = 1 - u - v$. Thus, competition results in decreasing birth rates for increasing population densities and vice versa. The per capita death rate, $d$, is equal and constant for both types. Spatial migration of cooperators and defectors is determined by the diffusion constants, $D_C$ and $D_D$, and the diffusion operator $\nabla^2 = \partial_x^2 + \partial_y^2$, where $\partial_i$ denotes the shorthand notation for the partial derivative with respect to $i$. The spatial domain $\Omega$ is $L \times L$, where $L$ denotes the linear extension of space, unless otherwise specified. We only consider Neumann boundary condition (i.e., zero-flux boundaries).

***Derivation of payoffs.*** Public-goods games are played in randomly formed groups with a maximum size of $N$. Participants are sampled by interpreting the densities $u$ ($v$) as probabilities for drawing a cooperator (defector) and $w$ for failing to find a participant, respectively. Thus, the population density, $u + v$, determines the effective interaction group size $S$ with an average size of $(u + v)N$. An individual finds itself in a group of size $S$ with probability

$$\binom{N-1}{S-1}(1-w)^{S-1}w^{N-S}.$$

In this group, the individual faces $m$ cooperators and $S - 1 - m$ defectors with probability

$$\binom{S-1}{m}\left(\frac{u}{u+v}\right)^m\left(\frac{v}{u+v}\right)^{S-1-m}$$

and the payoff for defectors and cooperators is given by

$$P_D(S) = \frac{r}{S}\sum_{m=0}^{S-1}\binom{S-1}{m}m\left(\frac{u}{u+v}\right)^m\left(\frac{v}{u+v}\right)^{S-1-m} \quad \text{[S2a]}$$

$$P_C(S) = P_D(S) + \frac{r}{S} - 1. \quad \text{[S2b]}$$

For convenience, the costs of cooperation are set to $c = 1$. Averaging over all group sizes $S$ yields

$$f_i = \sum_{S=2}^{N}\binom{N-1}{S-1}(1-w)^{S-1}w^{N-S}P_i(S)$$

with $i = C$ or $D$ and reduces to

$$f_D = r\frac{u}{1-w}\left(1 - \frac{1-w^N}{N(1-w)}\right) \quad \text{[S3a]}$$

$$f_C = f_D - F(w) \quad \text{[S3b]}$$

$$F(w) = 1 + (r-1)w^{N-1} - \frac{r}{N}\frac{1-w^N}{1-w}. \quad \text{[S3c]}$$

The difference between the payoffs of cooperators and defectors, $F(w)$, is always positive for $r < 2$ such that defectors prevail. For $r > 2$, $F(w) = 0$ has a single and unique root $\hat{w} \in [0,1)$ (1). For $w > \hat{w}$, $F(w) < 0$ holds, and hence, cooperators thrive. A more detailed derivation and analysis is provided in refs. 2 and 3).

***Nonspatial dynamics.*** The dynamics in the absence of space (see Eq. **1** in the main text), which corresponds to Eq. **S1** without the diffusion terms $D_C\nabla^2 u$ and $D_D\nabla^2 v$) reduces to a set of ordinary differential equations (ODE) that can be analyzed in detail (3). This provides the basis for the analysis of the spatial system of partial differential equations (PDE) in Eq. **S1**. Here, we focus on the scenario with baseline birthrates $b \geq 1$ and the more interesting case with death rates $d < b$, such that defectors cannot survive in the absence of cooperators ($\partial_t v < 0$ for $u = 0$). In this case, the ODE admits 2 fixed points that are of particular interest: **O** and **Q**. The state **O** denotes the extinction of the population ($u = 0, v = 0$) and is always stable. The existence and stability of **Q**, where cooperators and defectors can coexist, depends on the multiplication factor of the public good, $r$, but the thresholds of $r$ are analytically inaccessible because $\hat{w}$ cannot be determined for arbitrary $N$. However, it can be shown that **Q** is unique, if it exists (3). A lower bound for the existence of **Q** is given by $r > 2$ because otherwise $\hat{w}$ does not exist. At $r_{\text{Hopf}}$, the system undergoes a subcritical Hopf bifurcation (4) that gives rise to unstable limit cycles for $r$ close to but above $r_{\text{Hopf}}$. Note that with $b \geq 1$, supercritical Hopf bifurcations accompanied by stable limit cycles are impossible (3). For $r < r_{\text{Hopf}} = 2.3658$, **Q** is unstable and **O** is globally stable (numerical values are provided for the parameters used in all figures, $N = 8$, $b = 1$, $d = 1.2$). For $r_{\text{Hopf}} < r < r_2 = 6.53$, **Q** is stable, and the basin of attraction increases with $r$ but remains limited. For unfavorable initial configurations, either because of low population densities that result in a shortage of interaction partners [as described by the Allee effect (5)] or because of high relative abundance of defectors that diminish the public good, the population cannot recover and goes extinct, i.e., converges to **O**. Finally, for high multiplication factors, $r > r_2$, defectors disappear and cooperators thrive unchallenged.

## Spatial Dynamics

Selection and diffusion in spatial ecological public-goods games can trigger spontaneous pattern formation through diffusion-induced instability (Turing instability) or diffusion-induced coexistence. The heterogeneous density distributions of cooperators and defectors can be static, quasistatic with intermittent bursts of rapid changes or dynamic patterns of spatiotemporal chaos. The different dynamical regimes are summarized in a schematic phase plane diagram, Fig. S1.

**Diffusion-Induced Instability.** If the coexistence equilibrium **Q** exists and is stable in the absence of spatial extension ($r > r_{\text{Hopf}}$), then diffusion can destabilize **Q** because the ecological public-goods game represents an activator–inhibitor system (6, 7) in the vicinity of **Q**. The Jacobian matrix **J** at **Q** is given by

$$J = \begin{pmatrix} J_{11} & J_{21} \\ J_{12} & J_{22} \end{pmatrix} = \begin{pmatrix} -u\frac{d}{w} + uw\partial_u f_C & -u\frac{d}{w} + uw\partial_v f_C \\ -v\frac{d}{w} + vw\partial_u f_D & -v\frac{d}{w} + vw\partial_v f_D \end{pmatrix}. \quad \text{[S4]}$$

The fitness of cooperators and defectors is determined by their performance in public-goods interactions and adjusted by the population density. Increasing population densities (and hence decreasing $w$) reduces the fitness, which is reflected in the negative first term in each component of **J**. The second term indicates the effect of population densities on the payoffs. It is easy to see that increasing the defector density reduces the payoffs of both cooperators and defectors, i.e., $\partial_v f_C < 0$ and $\partial_v f_D < 0$ (see Eq. **S3**. Thus, defectors act as inhibitors. Similarly, increasing the cooperator density increases the payoffs of both types, i.e., $\partial_u f_C > 0$ and $\partial_u f_D > 0$, which indicates that cooperators act as activators whenever the population densities are sufficiently low. An activator–inhibitor system requires $J_{1i} > 0$ and $J_{2i} < 0$ at **Q**.

In this case, diffusion induced instability (or Turing instability) occurs if inhibitors (defectors) diffuse faster than activators (cooperators). Various critical parameters can be calculated that determine the spatial pattern formation (6–8). In particular, we can derive the minimum ratio of the diffusion coefficients of inhibitors and activators, $D_D/D_C$, as well as the characteristic length scale, $l$, of the emerging patterns (see *Pattern formation process* below). Any spatial perturbation in the square domain $\Omega$ is decomposed into spatial modes

$$\cos\frac{n\pi x}{L}\cos\frac{m\pi y}{L}. \qquad \text{[S5]}$$

with spatial eigenvalues $k^2 = \pi^2(n^2 + m^2)/L^2$, where $n$,$m$ are integers. The linearlized temporal dynamics of each spatial mode is given by

$$\frac{d}{dt}\begin{pmatrix} u_k \\ v_k \end{pmatrix} = \left[ \mathrm{J} - k^2 \begin{pmatrix} D_C & 0 \\ 0 & D_D \end{pmatrix} \right] \begin{pmatrix} u_k \\ v_k \end{pmatrix}, \qquad \text{[S6]}$$

where $\begin{pmatrix} u_k \\ v_k \end{pmatrix}$ denotes deviations from **Q**. The dynamics is not necessarily stable even if it is stable against homogeneous perturbations (i.e., $n = m = 0$ or $k = 0$). The necessary and sufficient condition for instability is determined by **J**, $D_C$, $D_D$ and $k$. In particular, if we neglect the condition that $n$,$m$ should be integers, the minimum ratio of diffusion coefficient is given by

$$\frac{D_D}{D_C} > \frac{-2J_{21}+J_{12}+J_{11}J_{22}+2\sqrt{-J_{12}J_{21}\det \mathrm{J}}}{J_{11}^2}. \qquad \text{[S7]}$$

The minimum ratio must be >1. Numerically we obtain $J_{ij}$ to confirm that the system satisfies the conditions for activator–inhibitor dynamics and derive the threshold value for $D_D/D_C$ that is required for the spontaneous emergence of spatial patterns (see Fig. S1).

***Pattern formation process.*** The pattern formation process can be understood and analyzed in greater detail in a 1-dimensional spatial setting. The most unstable mode, $k^*$, (with the largest eigenvalue $\lambda_{k^*}$) determines the characteristic length scale, $l$, of the emerging patterns with $l = 2\pi/k^*$. $k^*$ is estimated by $d\lambda_k/dk = 0$ where

$$\lambda_k = \frac{1}{2}\left( J_{11} + J_{22} - k^2(D_C + D_D) + \sqrt{\begin{array}{l}(J_{11} + J_{22} - k^2(D_C + D_D))^2 \\ -4(\det \mathrm{J} - k^2(D_C J_{22} + D_D J_{11}) + k^4 D_C D_D)\end{array}}\right). \qquad \text{[S8]}$$

The analytic estimation of $l$ provides an excellent approximation of the characteristic scale for the observed patterns both in 1 dimension (see Fig. S2) and in 2-dimensional space (see Fig. 2*A* in the main text).

Starting from an initially homogeneous distribution with densities near **Q** and a small disturbance in the center, then the spreading of the disturbance nicely illustrates the pattern formation process (see Fig. S2). First the perturbation grows, and the densities of cooperators and defectors increases. Due to the higher diffusion rate of defectors, cooperators suffer in the adjacent regions on either side, which decreases the densities of both strategies. The low defector densities then enable cooperators still further away from the initial perturbation to thrive, which triggers an increase in both strategies. This process repeats until the boundaries are reached. The distance between subsequent density peaks (or valleys) depends on the diffusion coefficients, $D_C$, $D_D$, and indicates the characteristic length scale, $l$.

***Diffusion-induced coexistence.*** Diffusion-induced coexistence is closely related to diffusion-induced instability with the only difference being that the coexistence equilibrium **Q** is unstable in the absence of space ($r < r_{\mathrm{Hopf}}$). Consequently, any deviation from **Q** is amplified over time in an oscillatory manner until the population goes extinct and reaches the globally stable equilibrium **O**. In the vicinity of $r = r_{\mathrm{Hopf}}$, the system again exhibits an activator–inhibitor dynamics, and the analysis of the Jacobian **J** at **Q** remains the same. Indeed, cooperators behave as activators as long as $r < r_{\mathrm{Turing}} = 3.31$. However, the homogeneous mode ($k = 0$) is already unstable, and a linear analysis is less powerful for diffusion-induced instability. Only recently, diffusion-induced coexistence attracted increasing attention (9), but a rigorous analysis is lacking. Diffusion-induced coexistence is not restricted to static patterns but allows much richer dynamics, which include spatiotemporal chaos (see Fig. S1).

The detailed pattern formation process for diffusion-induced coexistence is again nicely illustrated when considering a 1-dimensional system with a homogeneous initial distribution with densities of cooperators and defectors near **Q** and a small disturbance in the center. The densities in homogeneous regions oscillate and approach extinction, **O**, but the disturbance spreads and establishes stable heterogeneous strategy distributions (see Fig. S3). The basic spreading of the disturbance is the same as for diffusion-induced instability (see Fig. S2), because in both cases, the propagation is driven by the activator-inhibitor dynamics. In addition, the instability of **Q** manifests itself near the front of the propagating disturbance in that defectors destabilize peaks of high cooperator densities and repeatedly split them into 2 peaks until the boundaries are reached, and a stable heterogeneous strategy distribution takes shape.

**Robustness of Results.** To support our claims that spatial pattern formation promotes cooperation, we verified the robustness of our results for different initial configurations as well as other numerical methods and domain shapes.

***Numerics.*** For the numerical integration of Eq. **S1**, the spatial domain is discretized by a square grid with an equal spacing of $dx$ in both dimensions, and the time evolution is determined by using the Crank–Nicholson method (10) in time increments $dt$. Results in the chaotic regime are particularly sensitive to numerical methods. To verify the robustness, the numerical integration shown in Fig. 1 of the main text was carried out for all combinations of $dx = 0.25, 0.4, 1.0, 2, 4$ and $dt = 0.001, 0.01, 0.1, 1$. No qualitative differences were found for any combination. In addition, we checked the results using a different method based on finite elements [Hecht F, Pironneau O, Le Hyaric A, Ohtsuka K (2007) Freefem++: Finite element method to solve partial differential equations. www.freefem.org] with different boundary shapes (see Fig. 4). Again, no qualitative differences were found.

***Initial configuration.*** Numerical integration of PDEs is often susceptible to changes in the initial configuration. To verify the robustness of the pattern formation, we carried out simulations using initial configurations with a homogeneous disk of equal densities of cooperators and defectors located in the center of vacant space (see Fig. S5) instead of heterogeneous distributions

of random cooperator and defector densities (see Fig. 4 in main text). The qualitative features of the dynamics and the characteristic patterns remain unchanged. Only the boundaries of the chaotic regime are slightly different, but this is not surprising because this regime is defined by its susceptibility with respect to small configurational changes.

***Patterns.*** In the absence of space, the basin of attraction of the coexistence equilibrium **Q** is determined by $r$. For $r \leq r_{\mathrm{Hopf}}$, **Q** is unstable, and the population invariably disappears (the extinction state **O** with $w = 1$ is globally stable). For $r > r_{\mathrm{Hopf}}$, **Q** is stable, and the basin of attraction increases with $r$, but **O** remains locally stable for any $r$. The dynamics of the nonspatial ODE is shown in Fig. S6*a*. Spatial extension and diffusion enlarge the basin of attraction of **Q** by forming heterogeneous strategy distributions. Because measuring the basin of attraction is challenging, we consider $r$ just below $r_{\mathrm{Hopf}}$ such that **O** is globally stable in the absence of space. Nevertheless, in the spatial system, cooperators and defectors coexist (see Fig. S6*b*) for a broad range of initial population densities. Thus, spatial extension sustains the population by maintaining cooperation through pattern formation.


1. Hauert C, De Monte S, Hofbauer J, Sigmund K (2002) Replicator dynamics in optional public goods games. *J Theor Biol* 218:187–194.
2. Hauert C, Holmes M, Doebeli M (2006) Evolutionary games and population dynamics: maintenance of cooperation in public goods games. *Proc R Soc London Ser B* 273:2565–2570.
3. Hauert C, Wakano JY, Doebeli M (2008) Ecological public goods games: cooperation and bifurcation. *Theor Pop Biol* 73:257–263.
4. Kuznetsov YA (2004) *Elements of Applied Bifurcation Theory* (Springer, New York).
5. Stephens PA, Sutherland WJ (1999) Consequences of the Allee effect for behavior, ecology and conservation. *Trends Ecol Evol* 14:401–405.
6. Murray J (2003) *Mathematical Biology II: Spatial Models and Biomedial Applications* (Springer, Berlin).
7. Segel LA, Jackson JL (1972) Dissipative structure: An explanation and an ecological example. *J Theor Biol* 37:545–559.
8. Turing AM (1952) The chemical basis of morphogenesis. *Phil Trans R Soc London Ser B* 237:37–72.
9. Baurmann M, Gross T, Feudel U (2007) Instabilities in spatially extended predator–prey systems: Spatio-temporal patterns in the neighborhood of Turing–Hopf bifurcations. *J Theor Biol* 245:220–229.
10. Press WH, Teukolsky SA, Vetterling WT, Flannery BP (1988) *Numerical Recipes in C* (Cambridge Univ Press, Cambridge, UK).

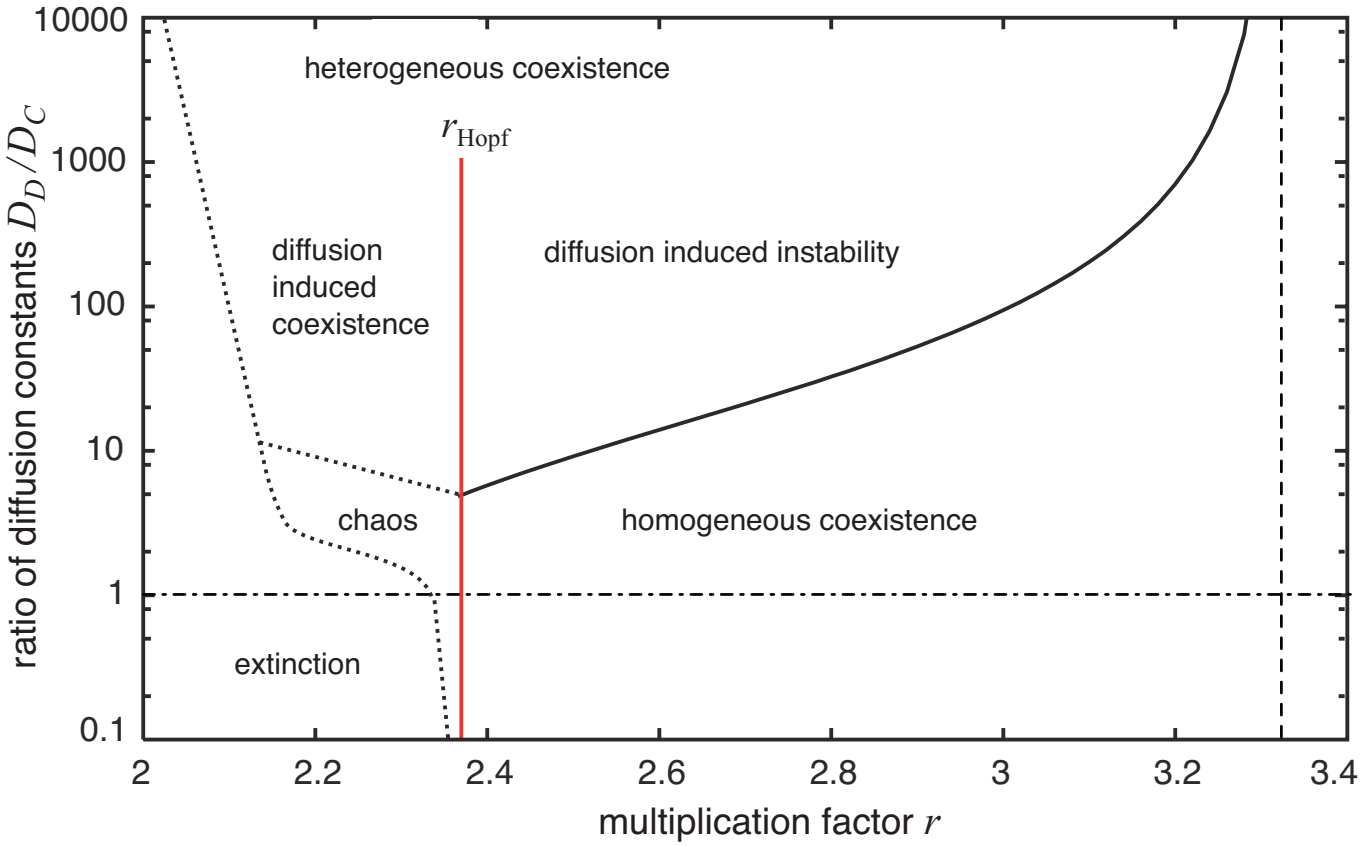


**Fig. S1.** Schematic phase plane diagram of the different dynamical regimes in terms of the ratio of the diffusion of defectors to cooperators, $D_D/D_C$ and the multiplication factor $r$ in spatial ecological public goods games. The vertical red line indicates $r_{\mathrm{Hopf}}$, which separates the region of extinction ($r < r_{\mathrm{Hopf}}$) and possible stable coexistence ($r > r_{\mathrm{Hopf}}$) in the absence of space. If cooperator diffusion exceeds defector diffusion, $D_D/D_C < 1$ the dynamics is barely affected by space, except for a small chaotic region near $r_{\mathrm{Hopf}}$. The dashed lines indicate approximate boundaries based on numerical results. These thresholds are analytically inaccessible and for the chaotic region even numerically challenging because the sensitivity of the system with respect to initial configurations increases when approaching the boundary of the parameter range where the population persists. The dynamics becomes much richer for $D_D/D_C > 1$. For $r < r_{\mathrm{Hopf}}$, the chaotic regime increases substantially and is replaced by diffusion-induced coexistence for high $D_D/D_C$. For $r > r_{\mathrm{Hopf}}$ the homogeneous spatial distributions are replaced by heterogeneous distributions triggered by diffusion induced instability (Turing patterns) for high $D_D/D_C$. The solid line indicates the analytical threshold ratio of the diffusion constants required for Turing patterns (see Eq. **S7**.) For very large $r > r_{\mathrm{Turing}} = 3.32$ (shown by the vertical dashed line) all patterns disappear. All thresholds refer to $N = 8$, $d = 1.2$, $b = 1$, $D_C = 1$ and are based on numerical integration using $L = 283$, $dx = 1.4$, $dt = 0.1$.

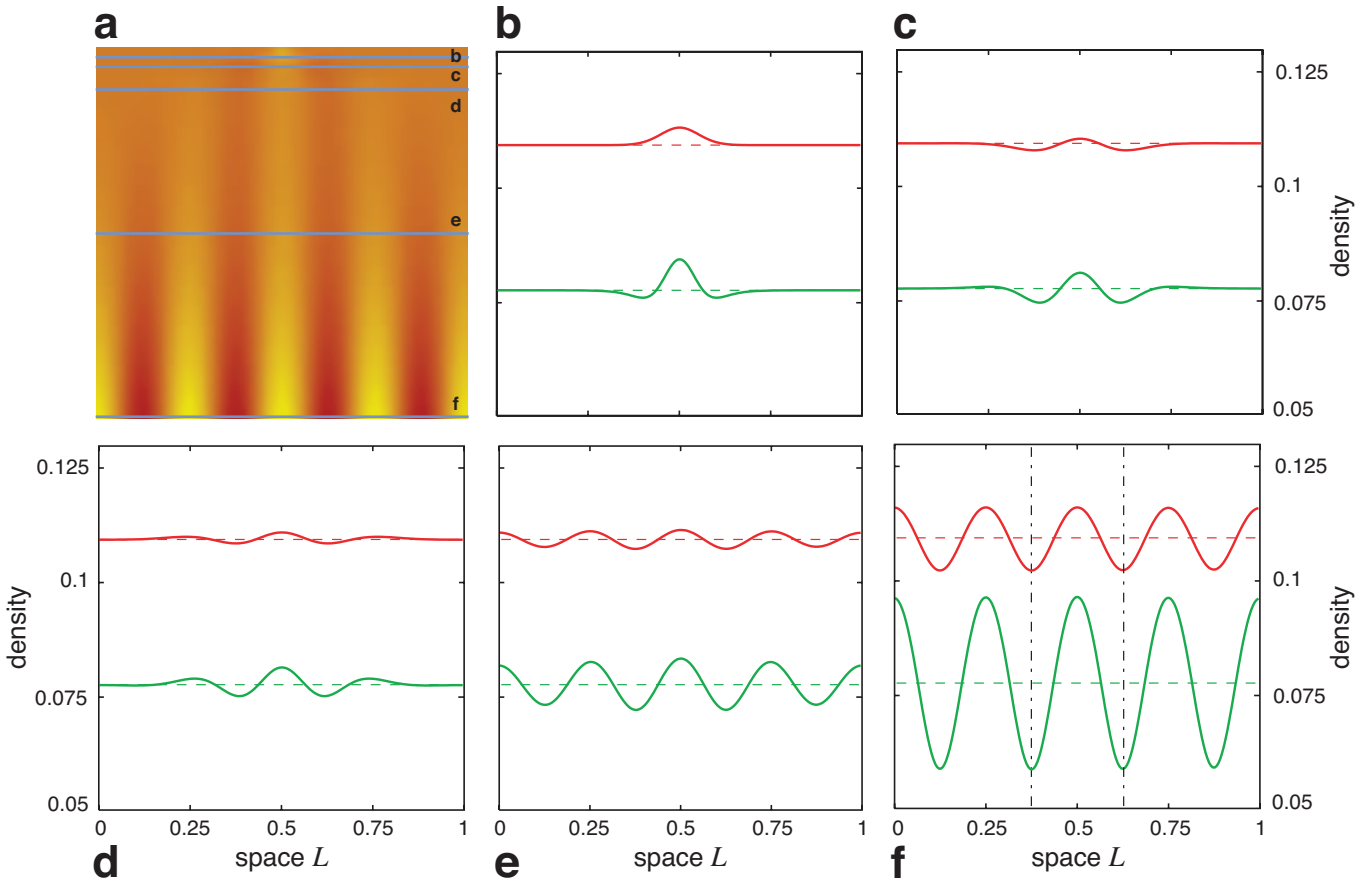


**Fig. S2.** Pattern formation process in ecological public goods games through diffusion-induced instability in 1-dimensional spatial systems. Initially the strategy distribution is homogeneous with densities near the stable coexistence equilibrium **Q** and a perturbation in the center (increase of the cooperator density by 0.1). (*a*) Space–time plot of the pattern formation process where the abscissa denotes space, and the ordinate the time (from top to bottom). The brightness of the colors indicates the density of cooperators (green) and defectors (red) or both (yellow). The horizontal lines in *a*, labeled b–f, indicate the times of the cross-sections of cooperator (green) and defector (red) densities in $t = 10$ (*b*), $t = 24$ (*c*), t = 40 (*d*), $t = 200$ (*e*), and $t = 398$ (*f*). In *b*–*f*, the dashed horizontal lines indicate the equilibrium frequencies of cooperators, $\hat{u}$, and defectors, $\hat{v}$ at **Q**. The dashed vertical lines in *f* indicate the characteristic length scale, *l*, according to Eq. **S8**. The game parameters are $N = 8$, $b = 1$, $d = 1.2$, $r = 2.5$, which yield $\hat{u} = 0.078$ and $\hat{v} = 0.11$. Diffusion coefficients are $D_C = 1$ and $D_D = 10$, spatial extension is $L = 100$ and numerical integration uses $dx = 0.5$ and time increments of $dt = 0.1$.

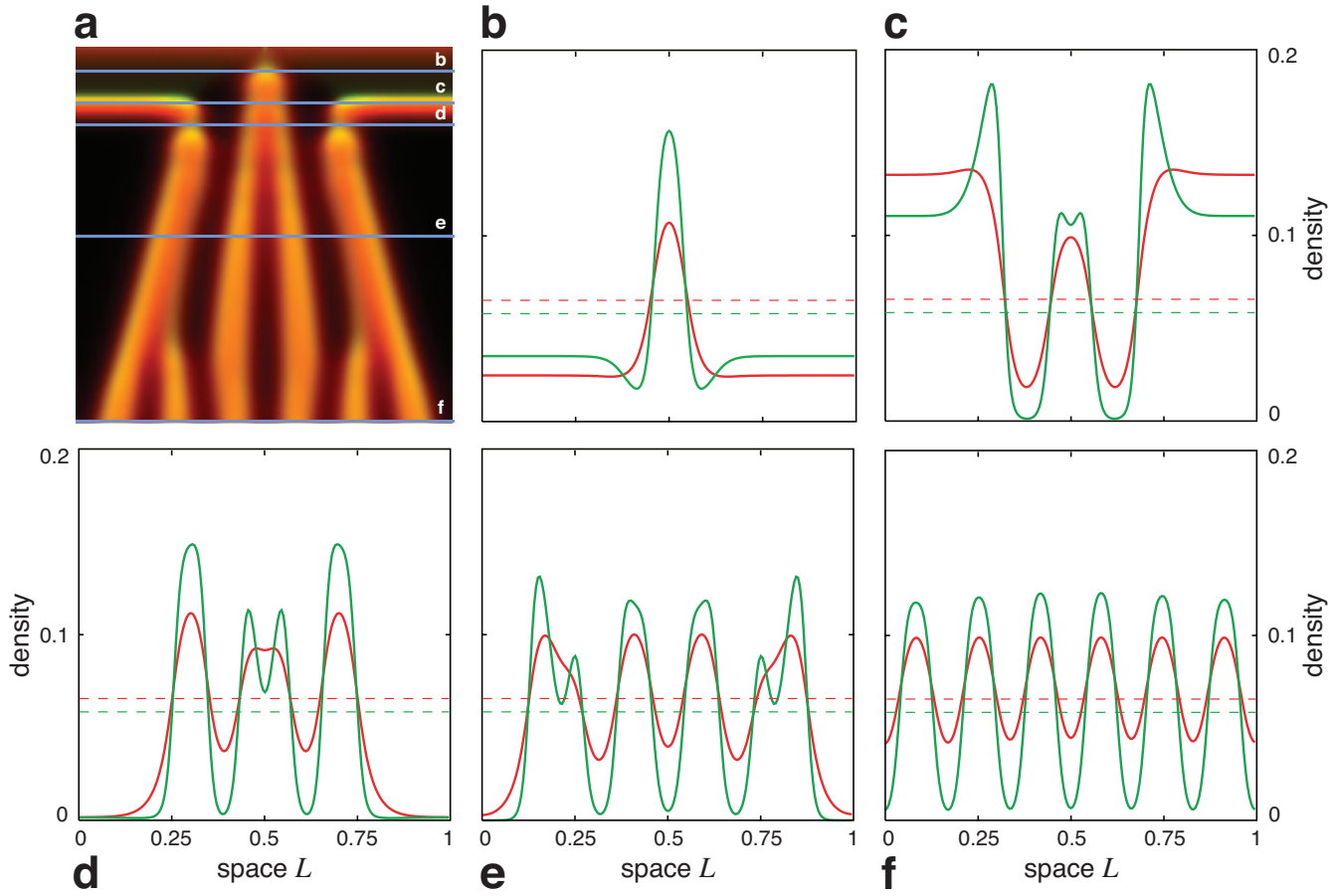


**Fig. S3.** Pattern formation process in ecological public goods games through diffusion-induced coexistence in 1-dimensional spatial systems. As in Fig. S2, the initial strategy distribution is homogeneous with densities near the unstable equilibrium **Q** and a perturbance in the center (increase of the cooperator density by 0.1). (*a*) Space–time plot of the pattern formation process where the ordinate denotes spatial extension and the abscissa the time (from top to bottom). The brightness of the colors indicates the density of cooperators (green) and defectors (red), both (yellow), or none (black). The horizontal lines in *a*, labeled b–f, indicate the times of the cross-sections of cooperator (green) and defector (red) densities $t = 30$ (*b*), $t = 60$ (*c*), $t = 99$ (*d*), $t = 300$ (*e*), and $t = 597$ (*f*). In *b*-*f*, the dashed horizontal lines indicate the frequencies of cooperators, $\hat{u}$, and defectors, $\hat{v}$ at the unstable **Q**. The game parameters are $N = 8$, $b = 1$, $d = 1.2$, $r = 2.3$, which yields $\hat{u} = 0.058$, $\hat{v} = 0.066$. Diffusion coefficients are $D_C = 1$ and $D_D = 10$, spatial extension is $L = 200$ and numerical integration uses $dx = 1$ and time increments of $dt = 0.1$.

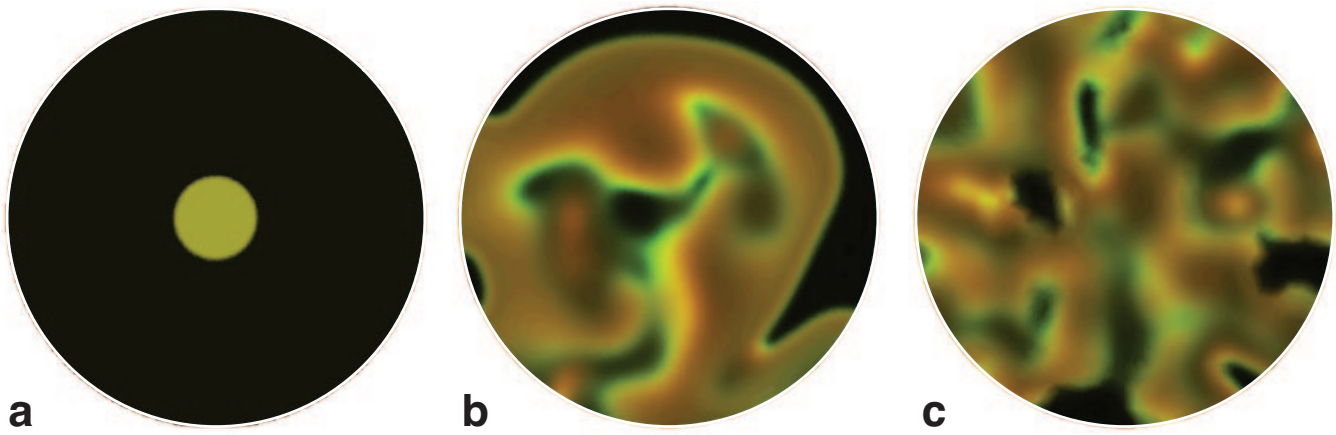


**Fig. S4.** Chaotic pattern formation in spatial ecological public goods. The setup is identical to Fig. 1 in the main text with the only differences that the spatial domain is circular instead of rectangular and the numerical integration of Eq. **S1** is based on the finite element method FreeFEM++ [Hecht F, Pironneau O, Le Hyaric A, Ohtsuka K (2007) Freefem++: Finite element method to solve partial differential equations. www.freefem.org]. The qualitative features of the emerging spatial patterns remain unchanged. (*a*) Initial configuration. (*b*) Snapshot at time $t = 2{,}000$. (*c*) Snapshot at $t = 7{,}000$. The parameters of the ecological public goods are $N = 8$, $d = 1.2$, $b = 1$, $r = 2.34$, $D_C = 1$, $D_D = 2$, and the initial configuration is a vacant disk with radius $R = 200$ (no flux boundary conditions) and a disk with radius $R/10$ in the center, where cooperators (green) and defectors (red) coexist at equal densities ($u_{disk} = v_{disk} = 0.1$ and $u = v = 0$ elsewhere).

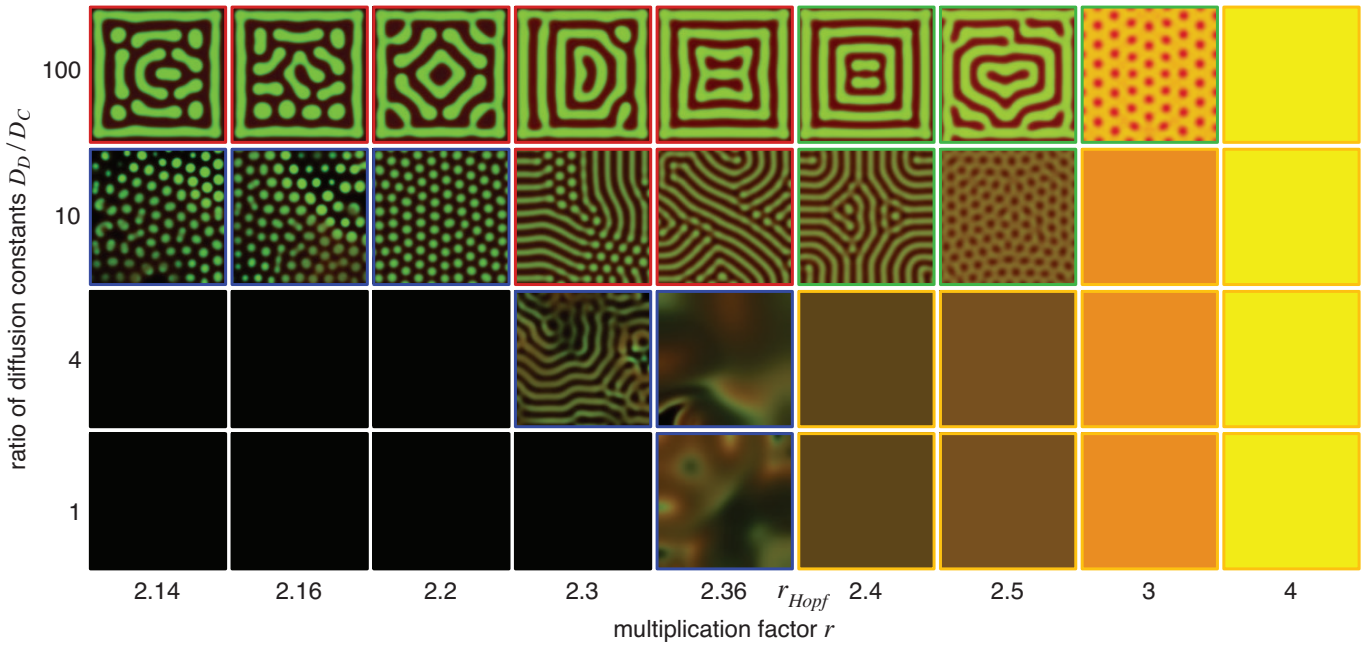


**Fig. S5.** Diversity of spatial distributions in terms of the ratio of the diffusion of defectors to cooperators, $D_D/D_C$, and the multiplication factor, $r$, in spatial ecological public goods games. This figure is identical to Fig. 4 in the main text with the only exception being that instead of a randomly mixed initial configuration, the initial state is given by a vacant $L \times L$ square and a homogeneous disk with radius $L/10$ in the center, where cooperators and defectors coexist at equal densities ($u_{\text{disk}} = v_{\text{disk}} = 0.1$ and $u = v = 0$ elsewhere; see Fig. 1 in the main text). The symmetry of the initial configuration leads to more symmetrical static patterns for diffusion induced instability (green frame) and diffusion induced coexistence (red frame). Homogeneous coexistence (yellow frame) remains unaffected. In all cases the qualitative features of the emerging strategy distribution remain unaffected by the initial configuration. Only the boundaries (but not the patterns) of the chaotic region (blue frame) are slightly shifted, but this is not surprising because chaotic dynamics is highly susceptible to perturbations. The parameters are $N = 8$, $d = 1.2$, $b = 1$, $D_u = 1$, $L = 283$, $dx = 1.4$, $dt = 0.1$, $r_{\text{Hopf}} = 2.3658$.

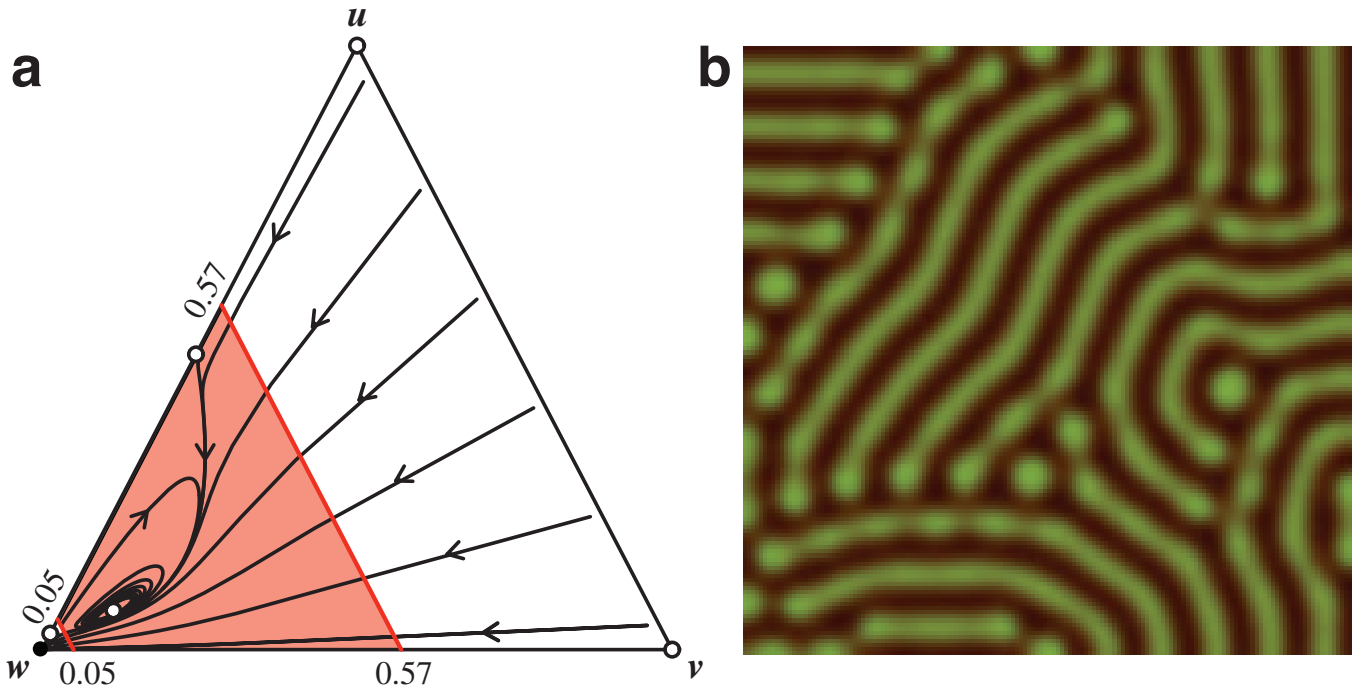


**Fig. S6.** Robustness of pattern formation in spatial ecological public goods games. (*a*) At or below the Hopf bifurcation, $r_{\text{Hopf}}$, extinction **O** is globally stable in the absence of space. (*b*) For the same parameters cooperators and defectors can coexist in a spatial setting through the spontaneous formation of heterogeneous strategy distributions. Diffusion stabilizes the unstable coexistence equilibrium **Q**. Qualitatively the same patterns emerge for different initial population densities, as indicated by the red area in *a*. Only for very low ($u + v < 0.05$) and for high ($u + v > 0.57$) population densities, coexistence is unreachable, and the population disappears just as in the absence of space. The density thresholds in *a* are numerically derived for $N = 8$, $r = 2.36$, ($r_{\text{Hopf}} = 2.3658$), $b = 1$, $d = 1.2$, $D_C = 1$, $D_D = 10$. The initial density, $p$, is fixed and we randomly set the cooperator density $u(x,y,0)$ according to a uniform distribution in $[0,p]$. The defector density is given by $v(x,y,0) = p - u(x,y,0)$. The time evolution for various $p$ determines the red area.

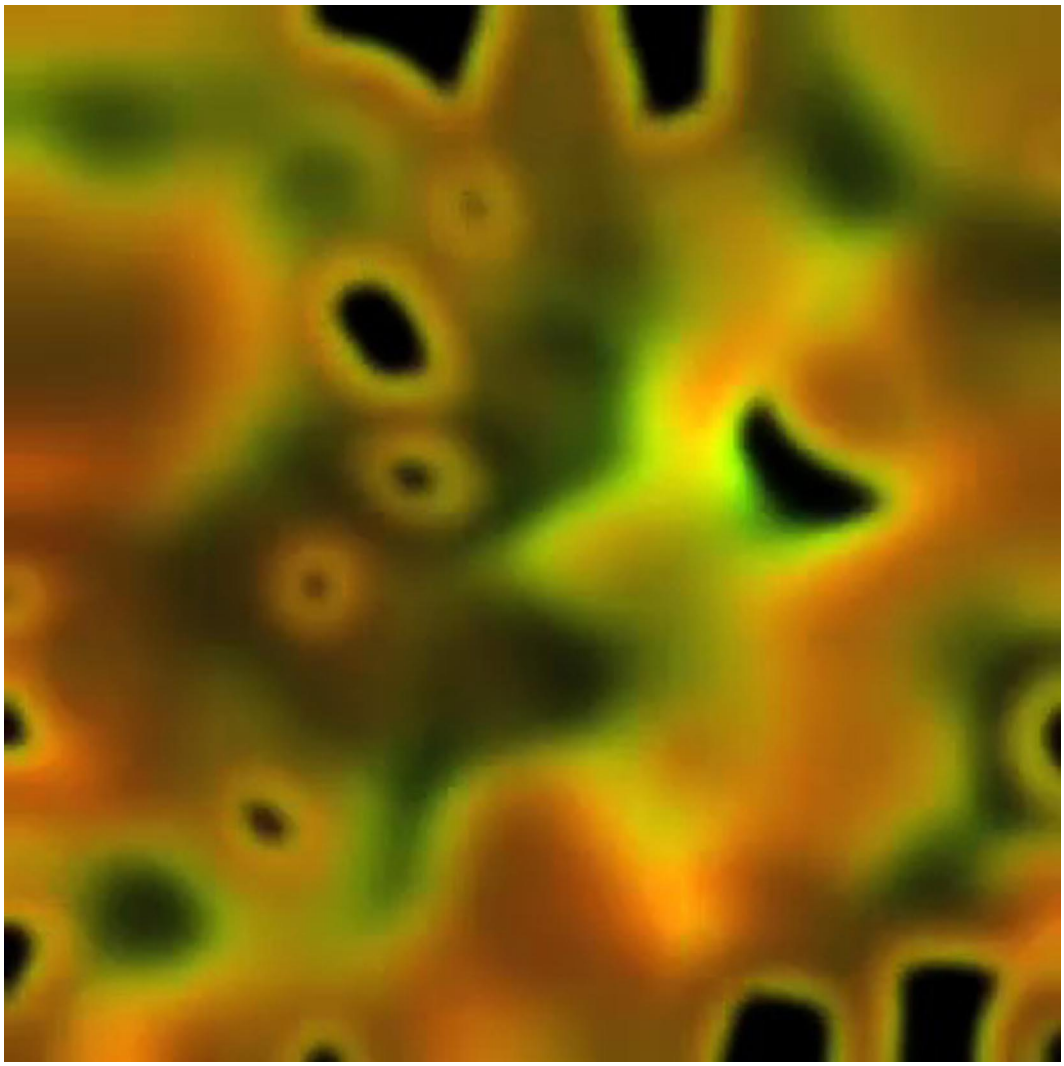

**Movie S1.** Spatiotemporal chaos. Onset of chaotic dynamics when starting from a symmetrical initial configuration (see Fig. 1 in main text). The deterministic dynamics should, in principle, preserve the symmetry, but it breaks down after some time because of limitations of the numerical integration combined with the exponential amplification of arbitrarily small deviations in chaotic dynamics. Parameters: $N = 8$, $r = 2.34$, $b = 1$, $d = 1.2$, $D_C = 1$, $D_D = 2$, $L = 400$, $dx = 0.8$, $dt = 0.01$ and the movie ends at time $T = 4{,}000$. The movies are highly compressed using the open standard H.264 and require QuickTime 7 or higher for playback.

Movie S1 (MOV)

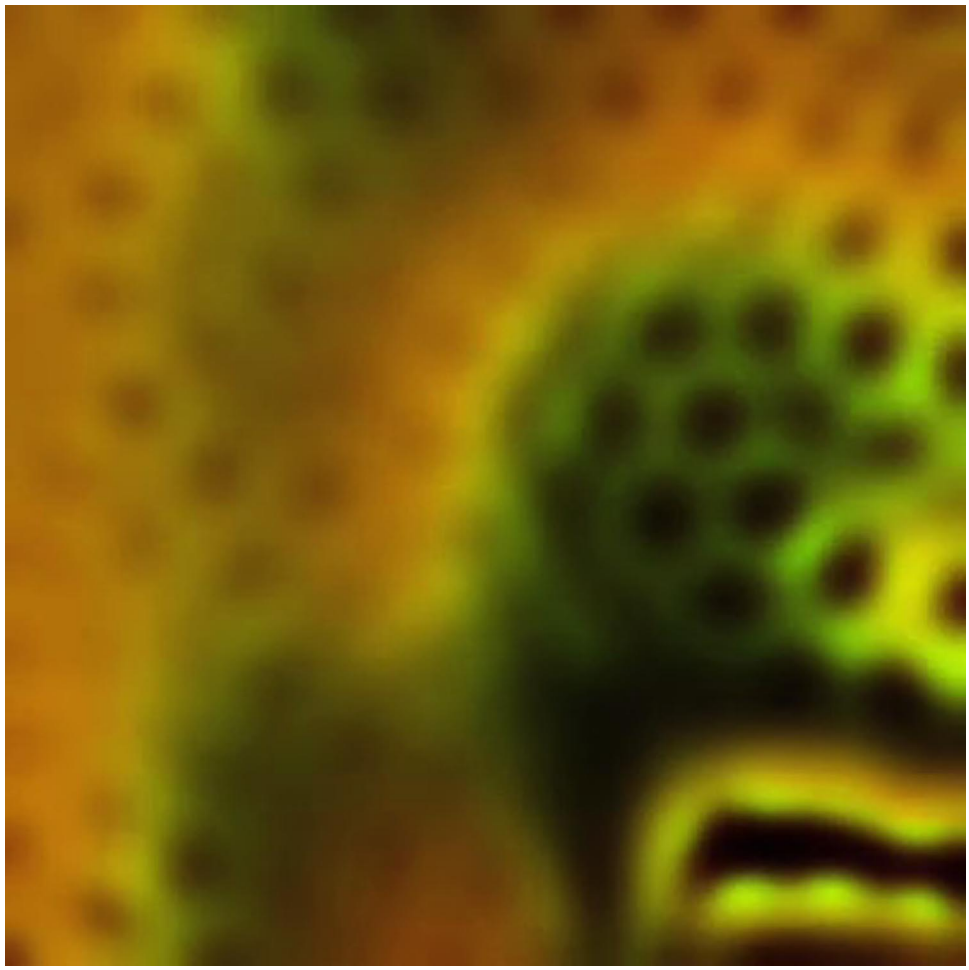

**Movie S2.** Intermittent activity. In the region of intermittent activity, the formation of quasistatic patterns alternates with rapid changes triggering local (or global) rearrangement and redistribution of cooperators and defectors. Parameters: $N = 8$, $r = 2.34$, $b = 1$, $d = 1.2$, $D_C = 1$, $D_D = 4$, $L = 256$, $dx = 0.8$, $dt = 0.01$ and the movie ends at time $T = 5{,}000$. The movies are highly compressed using the open standard H.264 and require QuickTime 7 or higher for playback.

Movie S2 (MOV)

**Movie S3.** Diffusion induced instability (Turing patterns). Cooperators and defectors form an activator–inhibitor system that destabilizes the homogeneous coexistence equilibrium **Q**. The antagonistic forces of cooperators (activators) and defectors (inhibitors) give rise to the formation of stable patterns. Parameters: $N = 8$, $r = 2.5$, $b = 1$, $d = 1.2$, $D_C = 1$, $D_D = 100$, $L = 256$, $dx = 0.8$, $dt = 0.01$ and the movie ends at time $T = 500$. The movies are highly compressed using the open standard H.264 and require QuickTime 7 or higher for playback.

Movie S3 (MOV)

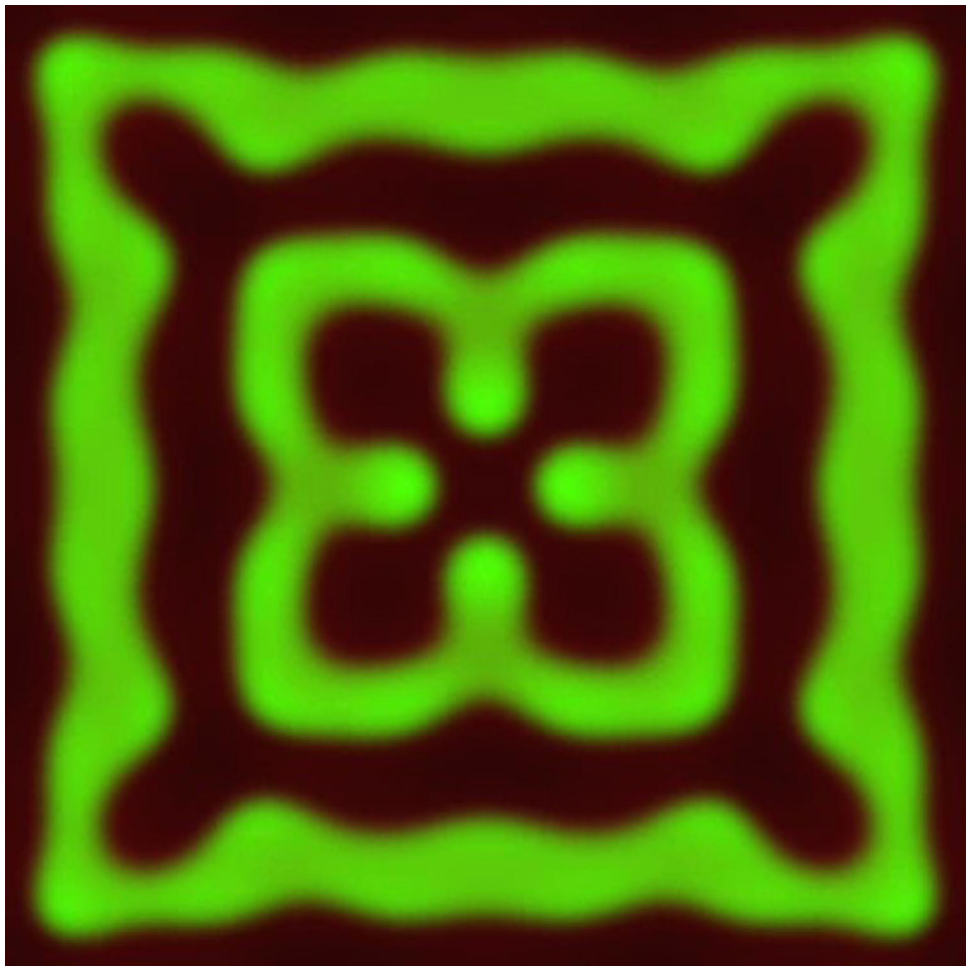

**Movie S4.** Diffusion induced coexistence. In the absence of space, the population goes extinct. The emerging spatial patterns are responsible for the survival of the population and permit stable coexistence of cooperators and defectors. Parameters: $N = 8$, $r = 2.2$, $b = 1$, $d = 1.2$, $D_C = 1$, $D_D = 100$, $L = 256$, $dx = 0.8$, $dt = 0.01$ and the movie ends at time $T = 2{,}000$. The movies are highly compressed using the open standard H.264 and require QuickTime 7 or higher for playback.

Movie S4 (MOV)